Coulomb Coupling and Heating of Charged Particle Beams in the Presence of Dispersion

Hiromi OKAMOTO[1)], Hiroshi SUGIMOTO[1)], Yosuke YURI[2)]

[1)] *Graduate School of Advanced Sciences of Matter, Hiroshima University*

1-3-1 Kagamiyama, Higashi-Hiroshima 739-8530, Japan

[2)] *Takasaki Advanced Radiation Research Institute, Japan Atomic Energy Agency*

1233 Watanuki-machi, Takasaki 370-1292, Japan

(Received: 28 August 2008 / Accepted: 28 October 2008)

We study heating of space-charge-dominated coasting beams circulating in a storage ring. A number of molecular dynamics simulations are performed systematically to figure out the parameter-dependence of the heating rate due to interparticle Coulomb collisions. The instability mechanism of interest to us here is basically the same as the so-called *radio-frequency heating* in a Paul trap. We introduce a new definition of the Coulomb coupling constant Γ that characterizes the phase of one-component plasmas. The new Γ is based on observable, averaged quantities and can be applied to dispersive situations. It is confirmed that the heating rate comes to a peak when the beam is in a liquid phase; the peak is always located at $\Gamma \approx 1$ regardless of particle species, beam energy, and line density.

Keywords: Coulomb coupling, charged-particle beam, storage ring, Coulomb crystal, beam emittance, thermodynamic temperature, momentum dispersion, rf heating, intrabeam scattering.

1. Introduction

A beam of charged particles traveling in an accelerator is typically in a *gaseous* state. Each particle oscillates about the reference orbit at high speed owing to the external focusing forces provided by a series of magnets. It is, however, possible in theory to bring the beam into the *liquid* or even the *solid* phase by applying a strong dissipative force. Such a procedure is called *cooling* because the beam temperature actually decreases in the center-of-mass frame. Recent progress in cooling and other accelerator technologies has made it more important to understand the behavior of high-density beams.

As is well-known, the dynamic motion of any beam is more or less influenced, mostly through Coulomb fields, by various surrounding objects such as vacuum chambers, radio-frequency (rf) cavities, counter-propagating beams, photo-electrons, etc [1]. In case these beam-environment interactions are weak and thus negligible, it is not difficult to recognize similarity between beams and non-neutral plasmas. We can actually prove that the collective motion of a beam is nearly equivalent to that of a one-component plasma confined in a compact trap system [2].

In this paper, we study the beam heating caused by Coulomb collisions among individual charged particles. Although the multi-particle system of interest to us here is moving at relativistic speed in the laboratory frame, the present discussion also applies to a non-neutral plasma in an rf trap because of their physical similarity mentioned above. The molecular dynamics (MD) technique is employed to evaluate the heating rates under various conditions. In each simulation, we start with an ultra-low temperature state where the beam is Coulomb crystallized, namely, in the solid phase. We then apply a perturbation and follow the temperature evolution to calculate the heating rate. As the temperature rises, the crystalline structure is destroyed and the beam eventually reaches an ordinary gaseous state. During this melting process, the collisional heating becomes maximum at relatively low temperature [3].

The paper is organized as follows: before proceeding to MD simulations, we describe the theoretical background of the present subject. In Section 2, brief discussions are made of ultra-cold beams and the temperature concept for later convenience. We then define, in Section 3, Coulomb coupling constants separately for the direction of beam motion and for the direction perpendicular to it. The new definition is based on the concept of *emittance* and somewhat generalized so as to tolerate the complication of the beam behavior due to momentum dispersion. Section 4 is devoted to showing MD simulation results obtained with various parameters. Concluding remarks are given in Section 5.

2. Ultra-low Temperature Regime

A charged-particle beam begins to show a complex collective behavior at higher density. Owing to Coulomb interactions that have a long range, the interparticle correlation becomes stronger as the beam is more compressed in phase space. Schiffer and co-workers first pointed out that a one-component plasma confined by a harmonic potential forms a spatially ordered configuration at ultra-low temperature [4]. Later, Wei, Li and Sessler demonstrated that such an order structure, now called a

author's e-mail: okamoto@sci.hiroshima-u.ac.jp

crystalline beam, can be stabilized even in a realistic storage-ring lattice that contains focusing and defocusing magnets, dipole magnets, and drift spaces [5]. At low line density, a *string* crystal is formed where particles are aligned along the reference orbit at equal intervals. By increasing the number of stored particles, we can convert the string into a *zigzag* structure and, eventually, into a *shell* structure [4,5]. These Coulomb crystals have already been realized in ion traps by means of laser cooling [6]. Similar strongly-coupled states can also be established in dusty plasmas [7]. As confirmed later, the rf heating is negligible in these ordered states because random Coulomb collisions are suppressed.

Despite many successful observations of Coulomb crystals in ion traps, nobody has succeeded in producing a crystalline beam in a real accelerator [8]. Several primary reasons why crystallizing a beam is so difficult have been identified theoretically [5,9]. One of the most important reasons is associated with the essential difference between an ion trap and a storage-ring accelerator, that is, the existence of dipole fields in the latter system. In order to make the beam orbit closed, we need dipole fields that give rise to momentum dispersion [10]. Another serious obstacle toward beam crystallization is resonance instability [9]. Heating due to resonance can cause major trouble in almost all existing storage rings whenever a beam is strongly cooled. By contrast, it is generally quite easy to avoid this instability in ion traps.

So far, we have used the term "temperature" without deep consideration of its meaning. When an ensemble of charged particles is confined by uniform, time-independent external fields, the temperature T can simply be evaluated from the average kinetic energy; namely,

$$k_{\mathrm{B}}T_{\eta} \equiv \frac{\left\langle p_{\eta}^{2} \right\rangle}{2m} \quad (\eta = x, y, z), \tag{1}$$

where k_{B} is the Boltzmann constant, m is the particle mass, p_{η} is the kinetic momentum of a particle in η-direction, and $\langle X \rangle$ stands for taking the average of quantity X over all particles. Provided that the system is in equilibrium, the temperatures of the three degrees of freedom are equal; i.e., $T_x = T_y = T_z$. When the external restoring force received by a non-neutral plasma is time-dependent, the simple definition above no longer applies. Suppose a large Coulomb crystal in a Paul trap, for instance. Because of the rf confinement field, the crystalline structure breathes as a whole, which means that $\left\langle p_{\eta}^{2} \right\rangle$ is always non-zero. Note also that the amplitude of the periodic breathing oscillation grows in an outer shell; the temperature of a larger crystal thus becomes higher according to the definition (1). To avoid this ambiguity, we often pay attention to non-periodic components of particle motion [11,12]. Temperature actually corresponds to the energy of "random motion", so the contribution of "coherent motion" must be subtracted before calculating T. The fact that we define the beam temperature in the center-of-mass frame is, in one sense, based on this thoughts. (All particles in a beam are flowing toward the same direction at roughly the same speed. We, therefore, subtract this coherent component of the beam motion prior to the temperature calculation.)

3. Coulomb Coupling Constants

The strength of the correlation in an interacting multi-particle system can be estimated from the *Coulomb coupling constant* Γ, defined as the ratio of the average Coulomb energy to the average kinetic energy [13]:

$$\Gamma \equiv \frac{q^2}{4\pi\varepsilon_0 d} \cdot \frac{1}{k_{\mathrm{B}}T}, \tag{2}$$

where q is the charge state of the particle, and $2d$ is the average interparticle distance. The Coulomb coupling of an ordinary accelerator beam is usually very weak and thus $\Gamma \ll 1$. The beam comes in to the liquid phase at $\Gamma \approx 1$ and is crystallized when Γ exceeds around 170 [13]. An important question now is how to define T in Eq. (2) or, in other words, how to subtract the coherent component of beam motion. Although the effective temperature studied in Refs. [11] and [12] is relevant to the present purpose, it requires the information of the orbits of individual particles that are not observable in real experiments. Instead, we here employ root-mean-squared (rms) quantities that are basically observable and enable a quick estimate of T. In what follows, we assume a coasting beam circulating in a storage ring. A Cartesian coordinate system, moving together with the beam, is taken such that the z-axis coincides with the direction of beam propagation. The *effective* beam focusing forces in the two transverse directions (x and y) are set equal for the sake of simplicity; then, the cross section of an equilibrium beam is roughly round on average at low temperature.

3.1 Transverse degrees of freedom

The volume occupied by a beam in six-dimensional phase space $(x, y, z\,; p_x, p_y, p_z)$ is called *emittance* that is invariant in a non-dissipative collisionless system. It is possible to show that the emittance can directly be linked to the entropy that is a measure of randomness. This suggests a possibility of using the emittance concept for temperature definition. The rms emittance projected to the transverse x-direction can be given by

$$\varepsilon_x = \frac{4}{m\beta\gamma c}\sqrt{\left\langle x^2 \right\rangle \left\langle p_x^2 \right\rangle - \left\langle x p_x \right\rangle^2}, \tag{3}$$

where β and γ denote the Lorentz factors; namely, in the laboratory frame, the beam is traveling at the speed βc (with c being the light velocity) and the total energy of the reference particle is $m\gamma c^2$. The projected rms emittance ε_y of the y-direction is introduced in a similar way. The two emittances are equal, i.e. $\varepsilon_x = \varepsilon_y (\equiv \varepsilon_{\perp})$, when the beam is in equilibrium. For a one-component plasma in a trap, we simply put $\beta\gamma = 1$ in Eq. (3) [14].

The transverse rms emittance $\varepsilon_\perp$ becomes smaller and smaller as the beam approaches the solid phase. It is straightforward to prove that $\varepsilon_\perp$ is exactly zero in a perfect crystalline state (except for quantum noise) [15]. Considering these facts, we define the transverse beam temperature $\tau_\perp$ as follows:

$$k_{\mathrm{B}}\tau_\perp \equiv \frac{p_0^2}{8m}\left(\frac{\varepsilon_\perp}{a}\right)^2, \tag{4}$$

where $p_0 = m\beta\gamma c$ is the kinetic momentum of the reference particle, and $a = 2\sqrt{\langle x^2\rangle}$ corresponding to the rms dimension of the beam. If the particles are uniformly populated, a agrees with the radius of the beam boundary [16]. When the external force is time-independent, the equilibrium distribution of particles is upright in the transverse phase space and, then, $\langle xp_x\rangle = 0$. In that case, Eq. (4) becomes identical to the conventional definition in Eq. (1). The average interparticle distance is roughly $d = (3a^2/4N)^{1/3}$ where N is the line density of the beam. Making use of this and Eq. (4) in Eq. (2), we obtain the coupling constant

$$\Gamma_\perp = 8r_p\left(\frac{4N}{3a^2}\right)^{1/3}\left(\frac{a}{\beta\gamma\varepsilon_\perp}\right)^2, \tag{5}$$

where r_p is the classical radius of the particle.

3.2 Longitudinal degree of freedom

With regard to a one-component plasma confined in a regular trap, there is no substantial difference among the three degrees of freedom. Although the axial confinement force is generally static in a linear Paul trap, the Γ-definition parallel to Eq. (5) holds for that direction; all we have to do is to replace x and p_x by z and p_z respectively. In the case of circular accelerators, however, the situation is more complex due to the existence of dispersion that couples the longitudinal beam motion with the transverse. Besides, the longitudinal dimension $\sqrt{\langle z^2\rangle}$ is not well defined for a coasting beam.

To understand how the dispersion creates coherence in the beam motion, consider a coasting crystalline beam circulating in a storage ring. It is clear that all particles must have an identical revolution frequency in order to maintain the ordered structure. In addition, the closed orbits of individual particles never cross, which means that the path length of a radially outer particle is longer than that of an inner particle [9,17]. We thus conclude that the outer particle must travel slightly faster than the inner particle; in other words, the angular velocity rather than the linear velocity must be the same. This fact naturally leads us to the expectation that the particle distribution of a crystalline beam should be linear in x-p_z phase space (not in z-p_z phase space) [18]. Figure 1 is a MD simulation result that actually verifies this expectation. The ion distribution observed at a particular point of a storage ring has been plotted on z-p_z phase plane (left panel) and on x-p_z phase plane (right panel). Each dot represents a single $^{24}\mathrm{Mg}^+$ ion traveling at the kinetic energy of 35 keV. As an example, we assumed the lattice of the storage ring "S-LSR" that is in operation at Kyoto University [19]. The ring is composed of six dipole magnets and six pairs of quadrupole magnets. We see that the ions are aligned only in x-p_z phase space. This linear distribution is maintained all around the storage ring while its tilt angle varies periodically. For the definition of the longitudinal emittance $\varepsilon_\parallel$, therefore, we use the emittance projection on to x-p_z phase plane,

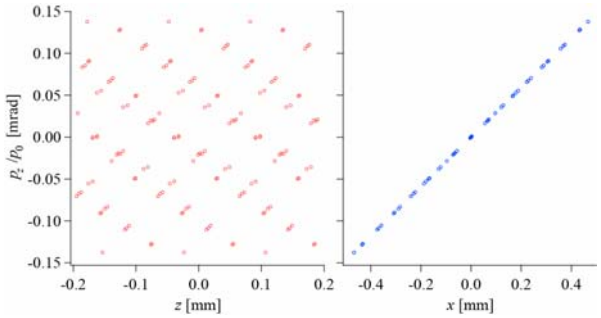

Fig.1 Typical phase-space distribution of particles forming a multi-shell crystalline beam in the storage ring "S-LSR". (a) z-p_z phase space, (b) x-p_z phase space.

$$\varepsilon_\parallel = \frac{4}{m\beta\gamma c}\sqrt{\langle x^2\rangle\langle p_z^2\rangle - \langle xp_z\rangle^2}. \tag{6}$$

With this rms quantity, $\tau_\parallel$ can be expressed, similarly to Eq. (4), as

$$k_{\mathrm{B}}\tau_\parallel \equiv \frac{p_0^2}{8m}\left(\frac{\varepsilon_\parallel}{a}\right)^2. \tag{7}$$

The longitudinal Coulomb coupling constant then takes the form

$$\Gamma_\parallel = 8r_p\left(\frac{4N}{3a^2}\right)^{1/3}\left(\frac{a}{\beta\gamma\varepsilon_\parallel}\right)^2. \tag{8}$$

4. Simulation Results

In order to explore the dynamic behavior of an ultracold relativistic beam in a particle accelerator, we developed the MD simulation code "CRYSTAL" that integrates the canonical equations of beam motion in a symplectic manner. The program is designed so that we can easily incorporate an arbitrary arrangement of various magnets sitting along the beam orbit. For the evaluation of interparticle Coulomb interactions, we employ the periodic boundary condition in the z-direction, slicing the coasting beam into many pieces of equal length; these *supercells* are assumed to have an identical particle distribution for computing efficiency. Short-range Coulomb interactions among individual particles are calculated in the reference supercell as precisely as possible, while we take the Ewald-type summation [20] over all supercells to make a quick estimate of the long-range Coulomb interactions [1].

It is well-known that the lattice of a storage ring must satisfy two primary conditions in order to achieve beam crystallization [5,9]. First, the ring has to operate below its transition energy. This requirement can easily be met in

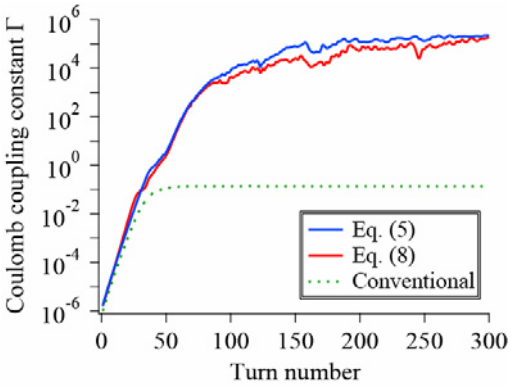

Fig.2 Time evolution of the transverse and longitudinal Coulomb coupling constants ($\Gamma_\perp$ and $\Gamma_\parallel$) during a cooling process. The dotted curve is based on the simple definition of temperature computed from the average kinetic energy as in Eq. (1).

practice by setting the design beam energy low. The second condition is associated with linear resonance, which has already been mentioned in Section 2. We must avoid this collective instability because the heating caused solely by Coulomb collisions is our concern here. In the course of our simulation study, we have employed several test rings satisfying these necessary conditions, and found no essential dependence of the results on the lattice designs. In the following, therefore, we only show MD results on S-LSR where the linear resonance can be eliminated by choosing proper parameters. The ion species assumed here is $^{24}Mg^+$ unless particularly noted. $^{24}Mg^+$ beams have actually been used in laser cooling experiments at S-LSR. The kinetic energy is adjusted to 35 keV well below the transition energy of the ring.

Typical time evolutions of the Coulomb coupling constants defined in Eqs. (5) and (8) are plotted in Fig. 2. The beam is initially so hot as usual that the Coulomb coupling is very weak before cooling. We then apply an ideal three-dimensional dissipative force to compress the beam in phase space. Both Γ's grow constantly, cross the threshold value of 170 beyond which the beam is actually crystallized, and finally exceeds 10^5. The line density assumed in this simulation is 4×10^5 m^{-1} where the resultant crystalline structure has three shells. For comparison, the coupling constant based on the simple average of squared momenta $\langle p_\eta^2 \rangle$ is indicated with a dotted line. Owing to the periodic breathing oscillations of the crystalline shells, the conventional Γ has been saturated at a very low level despite that the beam is certainly crystallized after about 70 turns around the ring. The saturation level is even lowered as the line density becomes higher.

We now show, in Fig. 3, the heating rates evaluated from MD data of different line densities. The same numerical data have been used for the plots in both panels, but the abscissas are different. In the upper panel, the abscissa is the transverse rms emittance ε_x given in Eq. (3) while the lower panel uses the transverse coupling constant $\Gamma_\perp$ in Eq. (5). We obtain similar pictures even if

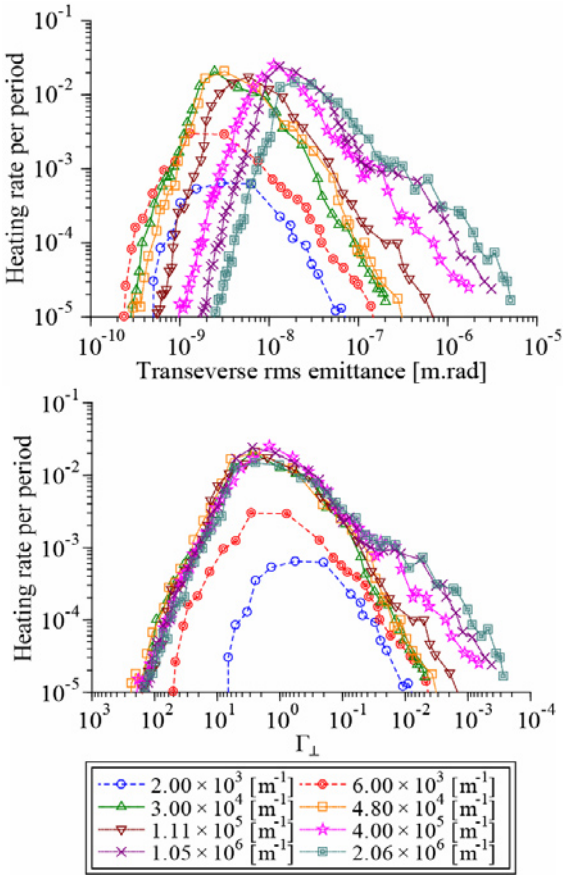

Fig.3 Dependence of the heating rate on beam line density. Identical MD simulation results have been plotted as a function of rms emittance ($\varepsilon_\perp$ in Eq. (3)) and as a function of Coulomb coupling ($\Gamma_\perp$ in Eq. (5)).

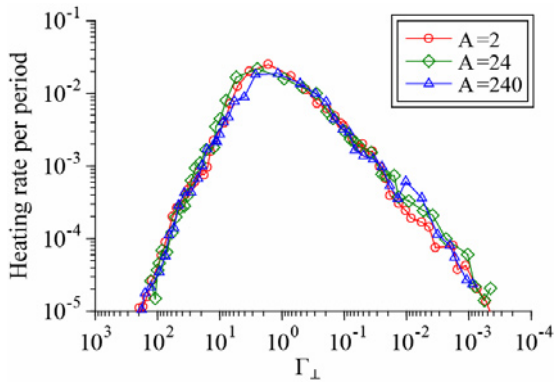

Fig.4 Dependence of the heating rate on ion mass. The line density of 2.37×10^5 m^{-1} has been assumed in the three examples.

$\varepsilon_\parallel$ and $\Gamma_\parallel$ are adopted as the abscissas. We confirm that the heating rate is extremely low in a crystalline state, which means that the ordered structure lasts very long even without artificial dissipation. To save the computing time, we weakly perturbed the crystalline state at the beginning and followed the temperature evolution. Then, the heating rate comes to a peak at relatively low temperature. The upper picture clearly indicates that the heating-rate mountain tends to shift toward the higher emittance side as the line density increases [21]. It is, however, reasonable to expect that collisions are most enhanced when the

Coulomb energy is comparable to the kinetic energy of particles, namely, in the region of $\Gamma \approx 1$. As verified in the lower picture, the peak position actually becomes almost independent of line density by plotting the heating rate as a function of Γ. The emittance-based temperature $\tau_\perp$ is also insensitive to line density and its value corresponding to $\Gamma \approx 1$ is about 0.1 Kelvin.

Similarly, we checked the dependence of the heating rate on ion mass number *A*, on beam energy, and on the strength of external confinement forces. It then turned out that the heating rate is always maximized at $\Gamma \approx 1$ regardless of mass number (as shown in Fig. 4) and beam energy. The peak position of the heating-rate curve, however, weakly depends on the plasma confinement strength; as the confinement force is increased, the peak generally moves toward the high Γ side.

5. Summary

We studied the beam emittance growth caused by interparticle Coulomb collisions. The MD simulation technique was employed to calculate the heating rate over the whole temperature range. The MD code developed for the present study enables us to simulate the dynamic motion of a charged-particle beam circulating in a storage ring of an arbitrary lattice structure. Through a number of systematic simulations, we found that the lattice details, if properly designed, is not essential to the heating behavior of the beam. It was verified that the heating rate is quite low at both ultra-low and high temperature ranges while it has a peak at relatively low temperature where the beam is in the liquid phase.

We introduced a new definition of temperature that is relevant to general situations where the external forces acting upon the beam are time-dependent and dispersive. The present definition requires no information of single-particle trajectories but is solely based on coarse -grained quantities. With this generalized temperature, the Coulomb coupling constants were defined as Eqs. (5) and (8) for the transverse and longitudinal directions. The dependence of the heating rate on various fundamental parameters was explored, which revealed that the peak heating usually occurs at $\Gamma \approx 1$. This conclusion should hold for nonneutral plasmas confined in ordinary trap systems such as a Paul trap.

References

[1] See, e.g., *Handbook of Accelerator Physics and Engineering*, edited by A. W. Chao and M. Tigner (World Scientific, Singapore, 1999).

[2] H. Okamoto and H. Tanaka, Nucl. Instrum. Meth. A **437**, 178 (1999).

[3] J. Wei and A. M. Sessler, Proc. European Particle Accel. Conf., 1179 (1996).

[4] A. Rahman and J. P. Schiffer, Phys. Rev. Lett. **57**, 1133 (1986); R. W. Hasse and J. P. Schiffer, Ann. Phys. (NY) **203**, 419 (1990).

[5] J. Wei, X.-P. Li and A. M. Sessler, Phys. Rev. Lett. **73**, 3089 (1994).

[6] R. P. Ghosh, *Ion Traps* (Oxford Science, Oxford, 1995), and references therein.

[7] H. Thomas, G. E. Morfill, V. Demmel, J. Goree, B. Feuerbacher, and D. Möhlmann, Phys. Rev. Lett. **73**, 652 (1994); J. H. Chu and Lin I, Phys. Rev. Lett. **72**, 4009 (1994); V. E. Fortov, A. P. Nefedov, O. F. Petrov, A. A. Samarian, and A. V. Chernyschev, Phys. Rev. E **54**, R2236 (1996); Y. Hayashi and K. Tachibana, Jpn. J. Appl. Phys. **33**, L804 (1994).

[8] Experimental evidence of the formation of "circulating" Coulomb crystals was reported previously in: T. Schätz, U. Schramm and D. Habs, Nature (London) **412**, 717 (2002). This excellent experiment is, however, based on a small circular Paul trap and the beam energy is only up to the order of 1 eV. Therefore, essential obstacles accompanied by high-energy beam experiments in real accelerators are negligible.

[9] J. Wei, H. Okamoto and A. M. Sessler, Phys. Rev. Lett. **80**, 2606 (1998).

[10] While dispersion is absent in *linear* beam-transport systems, it then becomes impossible in practice to employ the powerful laser cooling technique.

[11] J. D. Prestage *et al*., Phys. Rev. Lett. **66**, 2964 (1991).

[12] J. P. Schiffer *et al*., Proc. Natl. Acad. Sci. **97**, 10697 (2000).

[13] S. Ichimaru, Rev. Mod. Phys. **54**, 1017 (1982).

[14] H. Okamoto, S. Ochi and Y. Yuri, J. Phys. Soc. Jpn. **74**, 2099 (2005).

[15] H. Okamoto, Phys. Plasmas **9**, 322 (2002).

[16] Strictly speaking, the transverse temperature should be defined separately for the *x* and *y* directions. In fact, the projected emittances and average beam dimensions are not necessarily the same in both directions. We, however, consider the definition (4) here for simplicity, assuming a round cross section of the beam.

[17] H. Okamoto, Nucl. Instrum. Meth. A **532**, 32 (2004).

[18] In the transverse directions, particles form a straight line both in x-p_x and y-p_y phase spaces after a crystalline state is reached.

[19] A. Noda, Nucl. Instrum. Meth. A **532**, 150 (2004).

[20] P. P. Ewald, Ann. Phys. (Leipzig) **64**, 253 (1921).

[21] This is not necessarily the case at very low line density where the corresponding crystalline structure is a one-dimensional string.